S. Jegou, L. Barrallier, R. Kubler, M. A. J. Somers

Evolution of residual stress in the diffusion zone of a model Fe-Cr-C alloy during nitriding*

Ausbildung von Eigenspannungen in der Diffusionszone einer Fe-Cr-C Legierung während des Nitrierens

Abstract/Kurzfassung

Development and evolution of compressive residual stress during nitriding treatment are studied. A model carbon iron-based alloy Fe-3wt.%Cr-0.35wt.%C was nitrided in gas at 550 °C for different times. Microstructural investigation indicated an influence of the transformation and the associated carbon diffusion on the in-situ relaxation of residual stress induced by nitride precipitation. The transformation of initially present carbides into nitrides and the associated carbon accumulation ahead of the nitriding front is particularly taken into account. The distribution of residual stress in the nitrided case was predicted with a self-consistent mechanical model, using the volume changes associated with the phase transformations. To this end the nitrogen and carbon concentration distributions were converted into the equilibrium phase fractions of carbides and nitrides. An excellent correlation was obtained between experimental (X-ray diffraction analysis) and, thus, calculated independent residual stress distributions in the ferrite matrix. ■

Keywords: Nitriding, diffusion, precipitation, residual stress, relaxation, modelling

Es wurden die Entwicklung und Ausbildung von Druckeigenspannungen während einer Nitrierbehandlung untersucht. Die kohlenstoffeisenbasierte Legierung Fe-3wt.%Cr-0,35wt.%C wurde im Gas bei 550 °C und unterschiedlichen Haltedauern nitriert. Mikrostrukturuntersuchungen zeigten einen Einfluss der Umwandlung und der damit verbundenen Kohlenstoffumverteilung auf die Entspannung der von Nitridausscheidungen induzierten Eigenspannungen. Die Umwandlung der ursprünglichen Carbide in Nitride und die dadurch hervorgerufene Kohlenstoffanreicherung vor der Nitrierfront sind besonders berücksichtigt. Die Tiefenverteilung der Eigenspannungen in dem nitrierten Fall wurde mit einem selbstkonsistenten mechanischen Modell vorhergesagt, wobei die mit den Phasenumwandlungen verbundenen Volumenänderungen berücksichtigt werden. Zu diesem Zweck wurden die Stickstoff- und Kohlenstoff-Konzentrationstiefenprofile nach den Gleichgewichtsphasenanteilen der Carbide und Nitride umgerechnet. Es wurde eine ausgezeichnete Übereinstimmung zwischen experimentellen (Röntgenbeugungsanalyse) und theoretischen Eigenspannungsprofilen erhalten. ■

Schlüsselwörter: Nitrieren, Diffusion, Abscheidung, Eigenspannung, Spannungsabbau, Modellierung

Authors/Autoren: ***Dr. Sébastien Jegou,*** MécaSurf Laboratory, Arts & Métiers ParisTech, Aix-en-Provence, France; Technical University of Denmark, Dept. Mechanical Engineering, Kgs. Lyngby, Denmark, Jegou_Sebastien@yahoo.fr (Corresponding author/Kontakt)

Prof. Laurent Barrallier, Dr. Régis Kubler, MécaSurf Laboratory, Arts & Métiers ParisTech, Aix-en-Provence, France

Prof. Marcel A. J. Somers, Technical University of Denmark, Dept Mechanical Engineering, Kgs. Lyngby, Denmark

1 Introduction

Nitriding is a well-established thermochemical surface treatment of steels that highly enhances mechanical performance with respect to fatigue and corrosion [1]. The treatment relies on the precipitation of submicroscopic nitrides MN (M = Cr, V, Mo…), that significantly increases the hardness as well as involves the generation of compressive residual stress as a consequence of the accompanying volume expansion [2, 3]. For aeronautical applications, treated parts as bearings and turbine shafts require an appropriate combination of mechanical properties in the surface and in the core. Generally, steels containing nitride formers (e. g. 33CrMoV12-9 grade) are used and deeply nitrided up to 1 mm case depth [4]. Despite mechanical advantages, such treatments generally involve (at least) one hundred hours of nitriding, thereby increasing the risk for detrimental loss of surface properties due to mechanical relaxation. For instance, relax-

ation of compressive residual stresses close to the surface could occur [5]. This phenomenon, treated at the macroscopic scale, is generally attributed to the growth/coarsening of precipitates in the case of binary iron-based alloys or thermally controlled creep phenomena in the case of steels [6-8]. However, experimental investigations were neither able to identify dislocation production (except at precipitate/matrix interface) nor the occurrence of plastic straining [3, 9]. Relaxation of residual stress close to the surface was also phenomenologically linked to the development of cementite along grain boundaries more or less parallel to the surface [10]. Cementite develops as a consequence of the conversion of carbides into nitrides. The thus released carbon atoms diffuse either towards the surface, where they in principle can react to volatile components and leave the component, or diffuse deeper into the material, leading to the aforementioned cementite precipitation along grain boundaries [8, 11, 12]. The present work aims to study the role of carbon diffusion to larger depth on the development of the residual stress distribution during nitriding. To this end a model alloy Fe-3wt.%Cr-0.35wt.%C was taken as a reference. Details of the experimental investigations and mechanical modelling have been published elsewhere [13, 14].

2 Experimental

Samples of dimensions 27 mm x 27 mm x 30 mm were taken from a model Fe-3wt.%Cr-0.35wt.%C alloy, which was first austenitized at 830 °C, water quenched and annealed at 590 °C [13]. Gaseous nitriding was carried out at 550 °C for 10 h, 50 h and 100 h at a nitrogen potential that allows control of the compound layer thickness (details of the gas atmosphere are proprietary). Nitrogen and carbon content-depth profiles were determined by electron probe microanalysis (EPMA) in cross sections as well as by glow discharge optical emission spectrometry (GDOES) [13].

For microstructure investigation reflected light microscopy as well as scanning (SEM) and transmission electron microscopy (TEM) were applied; TEM specimens were prepared using focused ion beam (FIB) milling until electron transparency [13].

Residual stresses in the ferrite matrix were determined by investigating the {211} lattice spacing of α-iron by X-ray diffraction (XRD) using Cr-Kα radiation. The $\sin^2\psi$ method was used and combined with repeated electro-chemical surface layer removal for depth profiling [15]. As a consequence of the multiphase nature of the samples, the residual stress values obtained in this way represent the diffraction-weighted σ_{xx}-σ_{zz} [16].

3 Results and Interpretation

3.1 Morphology and composition

Optical micrographs in Figure 1 give an overview of the nitrided case after 10 h and 100 h nitriding. The precipitation of cementite along grain boundaries, inclined less than 45° with respect to the surface, is clearly revealed by using boiling picral as an etchant. Figure 2 gives back scattered scanning electron micrographs of the microstructure of the first 200 µm obtained after 10 h and 100 h nitriding at 550 °C. A porous compound layer of nearly 25 µm developed. Cementite along grain boundaries, inclined less than 45° with respect to the surface, is clearly revealed by backscatter electron imaging.

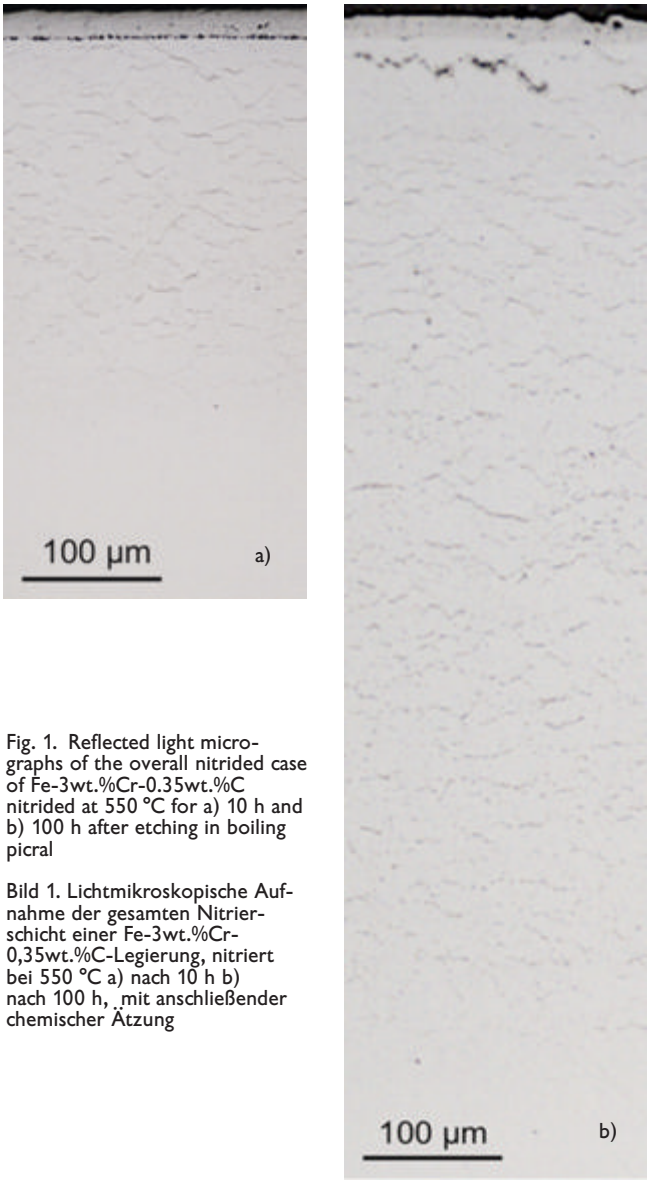

Fig. 1. Reflected light micrographs of the overall nitrided case of Fe-3wt.%Cr-0.35wt.%C nitrided at 550 °C for a) 10 h and b) 100 h after etching in boiling picral

Bild 1. Lichtmikroskopische Aufnahme der gesamten Nitrierschicht einer Fe-3wt.%Cr-0,35wt.%C-Legierung, nitriert bei 550 °C a) nach 10 h b) nach 100 h, mit anschließender chemischer Ätzung

After 100 h, γ'-Fe_4N nitride and porosity developed along grain boundaries in the diffusion zone at 25 µm to 80 µm depth, while cementite has disappeared in this region (Fig. 2b). X-ray diffraction confirmed the presence of Fe_4N nitride up to these depths [13]. A dark field TEM micrograph (selected area dark field of the ring in the diffraction pattern for the MN-nitrides) from a porous grain boundary at 50 µm depth is shown in Figure 3 and shows that γ'-Fe_4N has formed as a sheath around the porous boundary. Within the γ'-phase small alloying element nitrides are visible, which hints at the development of γ'-nitride after MN-nitride development. Since the presence of γ'-nitride in the diffusion zone is only associated with porosity along the grain boundaries, it is suggested that locally the pores along the ferrite grain boundary establish a direct connection with the gas mixture and, thus, the nitriding potential is applied at these locations leading to nitride formation. The observation of porous grain boundaries in the diffusion zone is consistent with the development of porosity in a similar Fe-Cr-C alloy during nitriding under conditions where no compound layer develops and where it was suggested that the porous boundaries are in direct contact with the gas atmosphere [8].

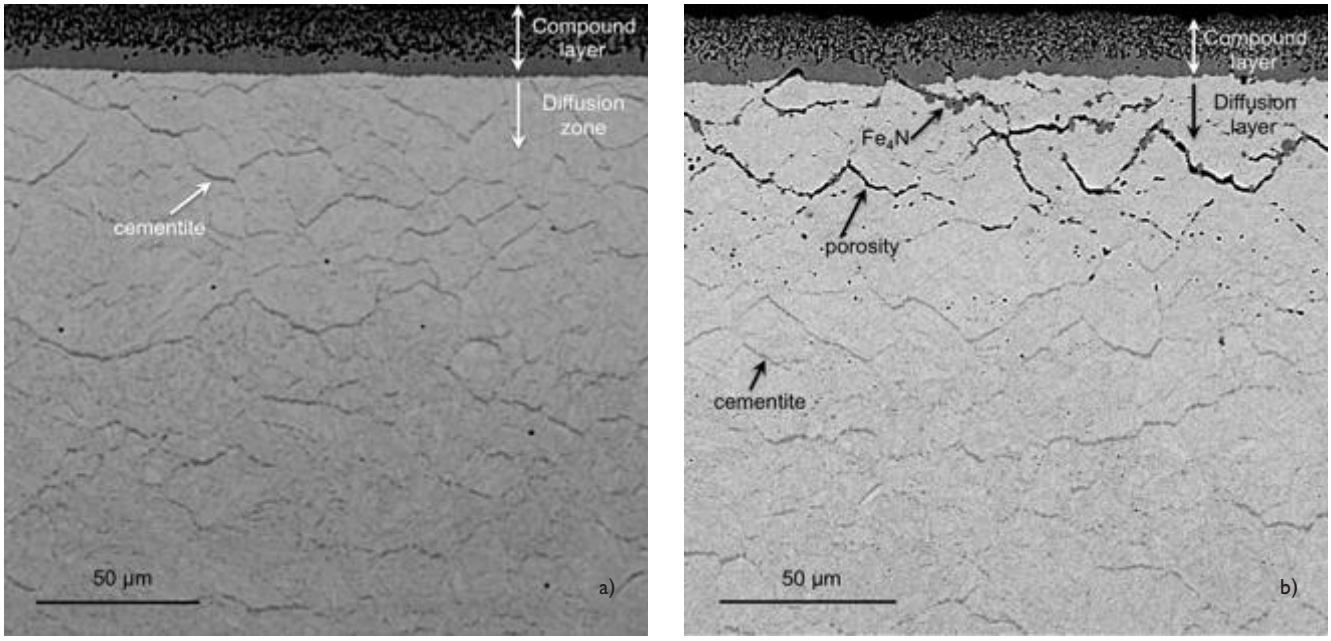

Fig. 2. Scanning electron micrographs (backscattered electron imaging) of unetched Fe-3wt.%Cr-0.35wt.%C nitrided at 550 °C for a) 10 h and b) 100 h

Bild 2. Rückstreu-elektronenmikroskopische Aufnahme einer geätzten Fe-3wt.%Cr-0,35wt.%C-Legierung, nitriert bei 550 °C a) nach 10 h und b) nach 100 h

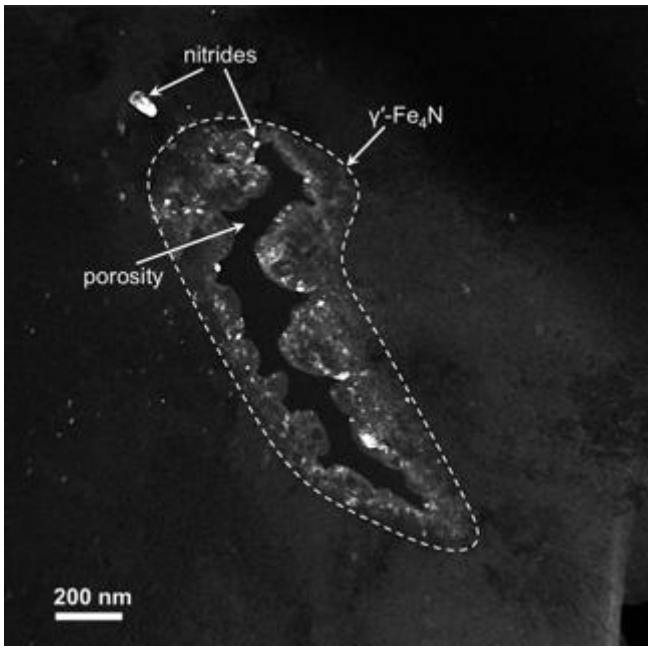

Fig. 3. FEM micrograph (dark field imaging) of Fe-3wt.%Cr-0.35wt.%C nitrided at 550 °C for 100 h at 50 µm depth. Dark field is taken for diffracted intensity from the ring belonging to MN nitrides

Bild 3. Transmissions-elektronenmikroskopische Aufnahme (helles Feld) einer Fe-3wt.%Cr-0,35wt.%C-Legierung, nitriert bei 550 °C nach 100 h in einer Tiefe von 50 µm

Composition-depth profiles determined with EPMA and GDOES are given in Figure 4. Clearly, within the nitrided case the nitrogen content decreases with depth and a relatively sharp case-core transition is obtained. Nitriding for 100 h under the given conditions brings about a diffusion zone reaching to a depth of approx. 900 µm. The carbon concentration decreases towards the surface and ahead of the nitriding front an accumulation of carbon is observed. On continued nitriding this carbon accumulation is pushed ahead of the nitriding front, showing that the carbides are dissolved or transformed during the prolonged uptake of nitrogen. Figure 5 compares the size distribution of carbides at a depth of 900 µm for the 100 h sample, where a carbon accumulation is observed, just ahead of the nitrogen diffusion front, with the carbide size distribution in the core of the steel. Clearly, the carbon pushed ahead of the nitriding front has led to growth of the equivalent diameter of the carbide particles, implying the incorporation of iron and, most likely also, alloying elements in the outer part of the carbides.

3.2 Residual stress

Residual stress distributions after 10 h, 50 h and 100 h of nitriding are shown in Figure 6. All profiles are characterized by a maximum compressive stress at some depth below the surface (175 µm, 450 µm and 550 µm for 10 h, 50 h and 100 h, respectively) and the occurrence of stress relaxation towards the surface. The value of the maximum compressive stress falls with nitriding time and its depth increases with nitriding time, consistent with [10]. At the beginning of the diffusion zone, tensile stresses were observed for 10 h and 50 h. Compressive stress had again developed after 100 h nitriding.

The depth of the diffusion zone is about 6 % of the half sample thickness. Hence, a reduction of the maximum compressive stress with depth cannot be ascribed to a distribution of stresses over case and core, but has to be attributed to microstructural changes.

According to the abovementioned observations, the following contributions to the evolution of the residual stress distribution in the nitrided case (and below) should be considered during nitriding:

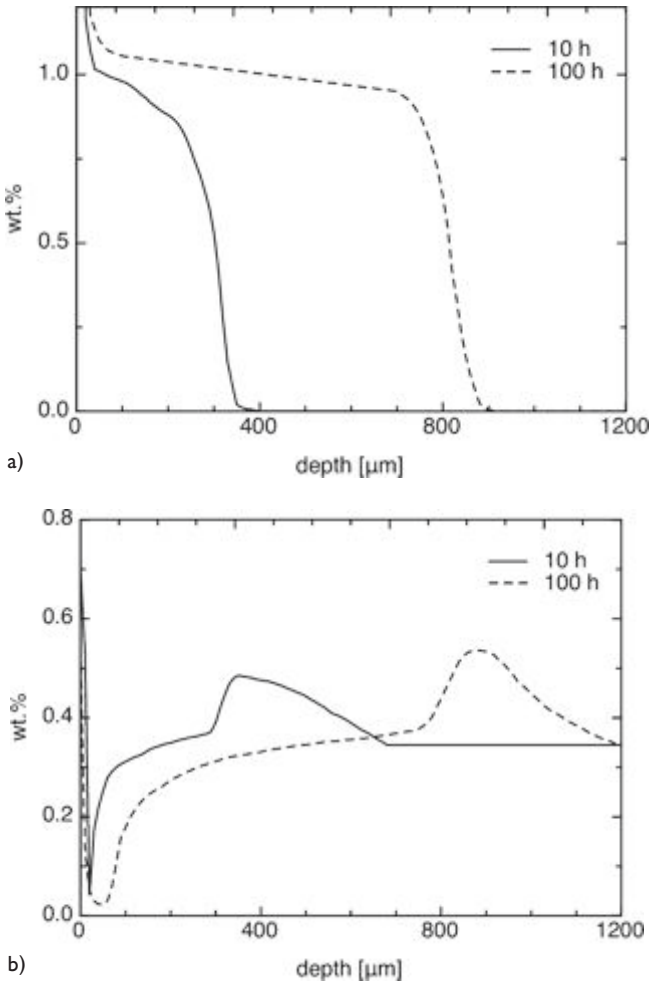

Fig. 4. Composition-depth profiles of Fe-3wt.%Cr-0.35wt.%C nitrided at 550 °C for 10 h and 100 h, a) nitrogen (EPMA analysis) and b) carbon (GDOES analyses)

Bild 4. Elementtiefen-Profile einer Fe-3wt.%Cr-0,35wt.%C-Legierung, nitriert bei 550 °C nach 10 h und 100 h, a) Stickstoff (ESMA-Analyse) und b) Kohlenstoff (GDOES-Analyse)

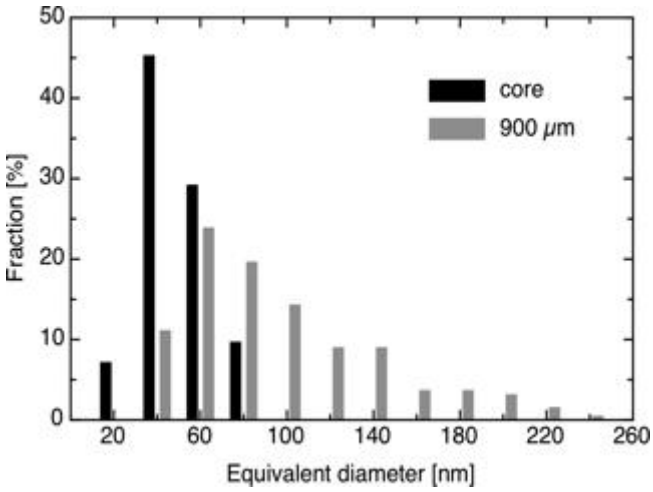

Fig. 5. Size distribution of precipitates found at a 900 µm depth (after 100 h nitriding) and within the core material. The total numbers of precipitates analysed are 188 and 236, respectively

Bild 5. Größenverteilung der Karbidausscheidungen in einer Tiefe von 900 µm (nach 100 h Nitrieren) und im Kern des Werkstoffs; die Gesamtzahl der analysierten Ausscheidungen beträgt 188 bzw. 236

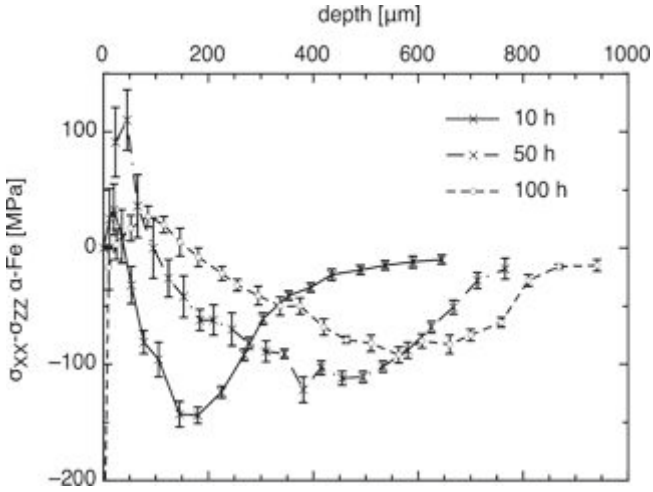

Fig. 6. Residual stress-depth profile in the ferrite phase of Fe-3wt.%Cr-0.35wt.%C nitrided at 550 °C for 10 h, 50 h and 100 h. The mean stress σ_{XX}-σ_{ZZ} was analysed by X-ray diffraction applying the $\sin^2\psi$ method

Bild 6. Eigenspannungs-Tiefenprofil in der ferritischen Phase der Fe-3wt.%Cr-0,35wt.%C-Legierung, nitriert bei 550 °C nach 10 h, 50 h und 100 h. Die Eigenspannungen σ_{XX}-σ_{ZZ} wurden mittels Röntgenbeugungsanalyse nach dem $\sin^2\psi$-Verfahren ermittelt

- development of alloying element nitrides from substitutional elements in solid solution. The nitrides have a larger specific volume than ferrite, which implies a volume increase accompanying nitride precipitation and involves the development of compressive residual stress in the diffusion zone.
- transformation of initially present carbides into alloying element nitrides is associated with a modest increase and thus lower compressive residual stress.
- precipitation of cementite along grain boundaries is most likely partly relaxed since preferably grain boundaries within 45° inclined to the surface are decorated to comply with the compressive residual stress associated with the finely dispersed alloying element nitrides. Thus the volume change accompanying the transformation is partly decreased.
- accumulation of carbon ahead of the nitriding front involves an increase of the volume fraction of carbides and a reduction of the alloying element content in solid solution in the ferrite matrix that would be available for finely dispersed nitride formation. Therefore, as compared to the surface adjacent region, deeper in the material the nitrides MN are less a consequence of the reaction between nitrogen and alloying elements dissolved in solid solution in ferrite, but are more a consequence of the transformation of carbides into nitrides. Since this transformation is associated with the development of cementite precipitation along grain boundaries, the overall volume change accompanying the precipitation of MN decreases, as does the compressive residual stress state.
- dissolution of cementite in the part of the diffusion zone close to the compound layer and the formation of porosity along grain boundaries provides a means for stress relaxation. The subsequent formation of γ'-Fe_4N is likely to be associated with a contribution to stress.

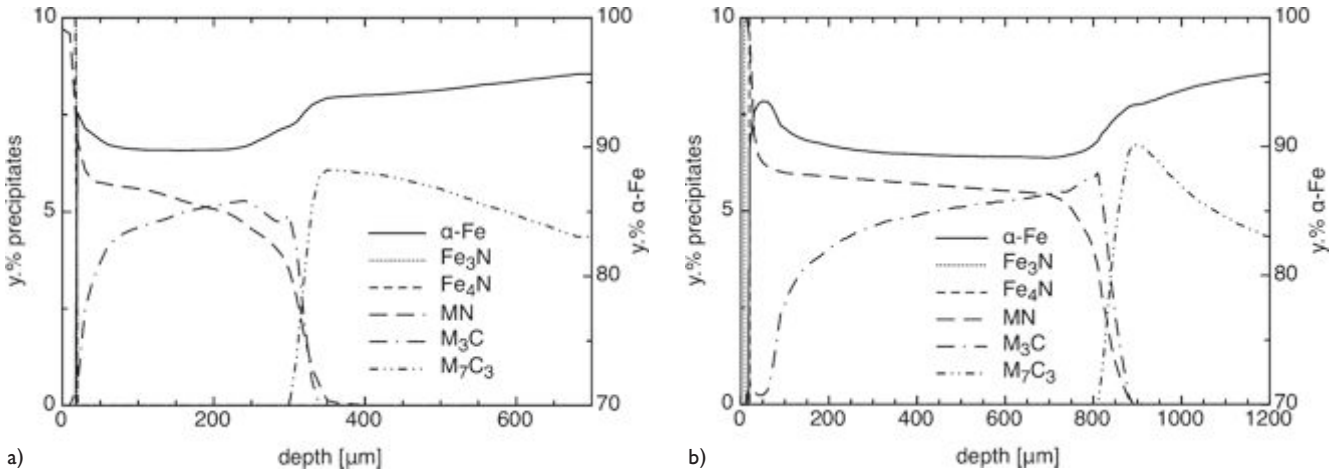

Fig. 7. Evolution of the equilibrium phase fractions in Fe-3wt.%Cr-0.35wt.%C nitrided at 550 °C for a) 10 h and b) 100 h. Results calculated with Thermo-Calc software from the composition-depth profiles in Fig. 4

Bild 7. Entwicklung des Phasenanteils in einer Fe-3wt.%Cr-0,35wt.%C-Legierung, nitriert bei 500 °C nach a) 10 h und b) 100 h; die Ergebnisse wurden mit Thermo-Calc aus dem Elementtiefenprofil in Bild 4 berechnet

4 Modelling

An attempt is provided to predict the distribution of residual stress from the microstructural changes in the material. To this end firstly the fractions of the phases present and their equilibrium compositions are calculated from the composition-depth profiles in Figure 4, using version R of Thermo-Calc software and SSOL2 thermodynamics database. In principle this approach could also include a simulation of the growth kinetics of the diffusion zone [17]. This was however not included in the present version, because residual stress affects the diffusion kinetics of interstitials to an unknown extent. The material is conceived as a semi-infinite volume element subdivided in sublayers over the depth of the case. The number of sublayers depends on the spatial resolution of nitrogen/carbon content-depth profiles obtained. Volume changes are considered relative to the carbon content and phase fractions in the core of the metal.

The mechanical part of the model is used to convert the phase fractions and the associated volume changes into residual stresses [14, 15]. In a first approximation, a system of randomly distributed precipitates within a matrix is idealized by an inclusion embedded in a ferrite matrix. At a given depth, the mechanical model is based on the self-consistent mechanics of heterogeneous materials [18]. When dealing with multi-scale heterogeneities as in case of a nitrided surface, such a model is more appropriate than a macroscopic approach using a classical mixture law.

The abovementioned semi-infinite volume is assumed homogeneous and isotropic within the small strain assumption. According to X-ray analysis, a macroscopic (i. e. involving all phases in the multiphase microstructure) state of plane stress is verified over the depth of the nitrided case depth.

Ferrite and precipitates are assumed to have elastoplastic and elastic behaviours, respectively. During diffusion and precipitation, the volumetric strain of the matrix is assumed negligible compared to the precipitates, i. e. all volume changes are associated with transformations in phases or the appearance of new phases.

Finally, for all depths the mean stresses σ_{XX}-σ_{ZZ} in the ferrite matrix as well as the macroscopic (overall) stresses are calculated in order to be able to compare with X-ray diffraction analysis. It has to be noted that lattice parameters of phases are composition (when known) and temperature dependent. More details of the calculations are provided in [14, 15].

4.1 Modelling results and discussion

Experimental nitrogen and carbon content-depth profiles from Figure 4 were used as input to calculate the phase fractions under presumed local equilibrium conditions at each depth. The results are presented in Figure 7, which gives the evolution of the equilibrium phase fractions over the case depth after 10 h and 100 h nitriding at 550 °C. Clearly, ThermoCalc predicts that during nitriding carbides of type M_7C_3 are replaced by nitrides of type MN and M_3C (cementite), which is largely in correspondence with the experimental observations. The carbon accumulation ahead of the nitriding front is associated with a higher fraction of carbides of type M_7C_3 (under equilibrium conditions), which is in agreement with growth of the fine carbides (Figure 5). The presence of γ'-Fe_4N along porous grain boundaries in the oldest part of the diffusion zone is not predicted by ThermoCalc. From the phase fractions (and the equilibrium phase compositions) the volume changes accompanying the transformations were calculated, using the specific volumes listed in Table 1. A maximum volume fraction of precipitates of nearly 10 % (Figure 8a) corresponds to a maximum volume change of 1.32 % and 0.86 % after 10 h and 100 h nitriding are obtained, respectively (Figure 8b). The changes are particularly significant in the part of the diffusion zone close to the compound layer, where the depletion of carbon and grain boundary porosity occur. The calculated residual stress distributions within the ferrite matrix after 10 h and 100 h nitriding are given in Figure 9 and compared to the experimental stress distributions determined with X-ray diffraction analysis (cf. Figure 6). A most encouraging quantitative agreement between the measured and calculated stress profiles is observed for the majority of the diffusion zone. It is noted explicitly that calculated and measured stress values are independent from each other and that the only experimental input for the model are the (independent) composition profiles of nitrogen and carbon over the nitrided case.

Phase	Structure	a [nm]	b [nm]	c [nm]	V [$cm^3.kg^{-1}$]
α-Fe	Cubic	0.28664	-	-	127.06
CrN	Cubic	0.4140	-	-	161.29
Fe_3C	Ortho.	0.50910	0.67434	0.45260	130.38
$Cr_{23}C_6$	Cubic	106.599	-	-	144.93
Cr_7C_3	Ortho.	0.7019	12.158	0.426	145.24
Fe_4N	Cubic	0.3791	-	-	138.89
Fe_3N	Hexa.	0.2695	-	0.4362	125.79

Table 1. Lattice parameters a, b, c and specific volume V of phases used in the present model of nitriding of steels. Data are taken from the JCPDS database [19]

Tabelle 1. Gitterparameter und spezifisches Volumen V in der vorliegenden Modellierung der Nitrierung (ICPDS-Datei) [19]

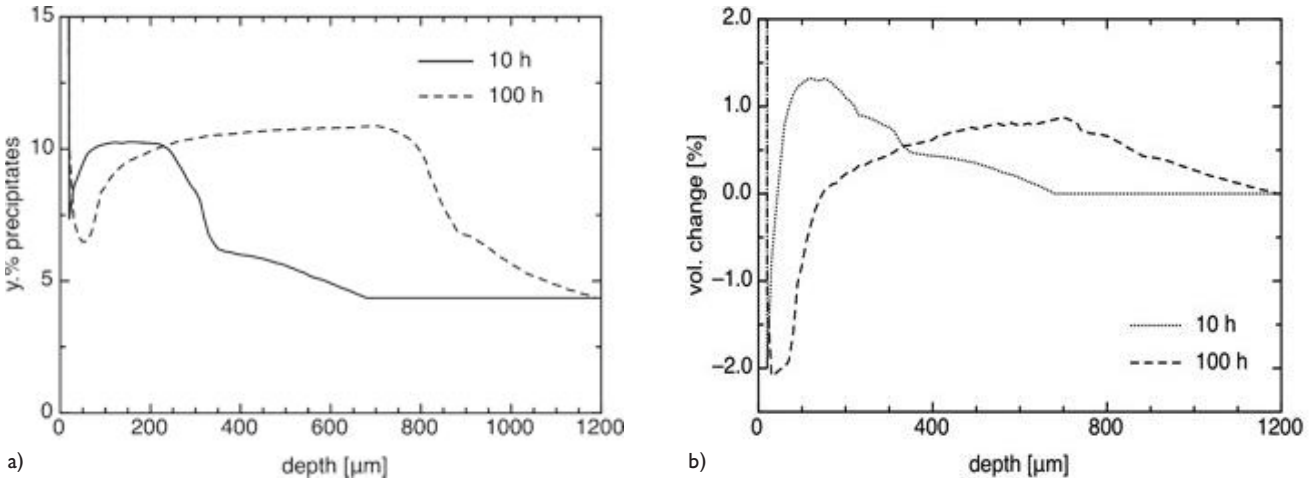

Fig. 8. a) Evolution of the overall volume fraction of secondary phases in Fe-3wt.%Cr-0.35wt.%C nitrided at 550 °C for 10 h and 100 h. Results calculated with Thermo-Calc software; b) calculated volume changes accompanying the secondary phases as compared to the initial state for nitriding of Fe-3wt.%Cr-0.35wt.%C at 550 °C for 10 h and 100 h

Bild 8. a) Entwicklung des Volumenanteils der Sekundärphasen einer Fe-3wt.%Cr-0,35wt.%C-Legierung, nitriert bei 550 °C nach 10 h und 100 h, Ergebnisse wurden mit Thermo-Calc berechnet; b) berechnete ausscheidungsinduzierte Volumenänderung in der Nitrierschicht im Vergleich zum Ausgangszustand der Fe-3wt.%Cr-0,35wt.%C-Legierung, nitriert bei 550 °C nach 10 h und 100 h

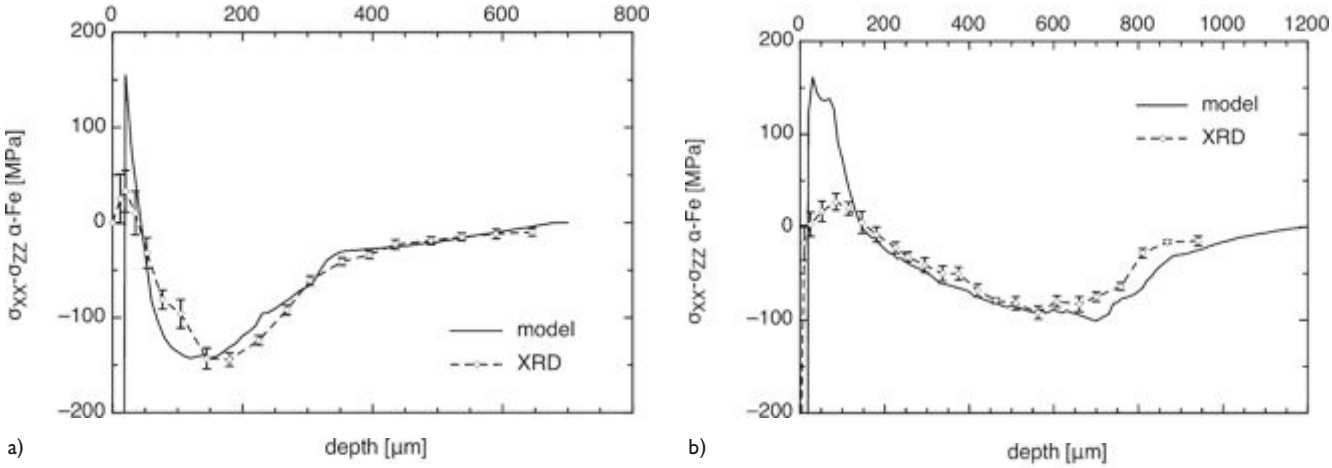

Fig. 9. Calculated residual stress profiles over the ferrite matrix of Fe-3wt.%Cr-0.35wt.%C nitrided at 550 °C for a) 10 h and b) 100 h, in comparison with X-ray diffraction analysis (cf. Fig. 6)

Bild 9. Berechnete Eigenspannungsverläufe in der ferritischen Matrix einer Fe-3wt.%Cr-0,35wt.%C-Legierung, nitriert bei 550 °C nach a) 10 h und b) 100 h im Vergleich zu den mit Röntgenbeugungsanalyse ermittelten Verläufe (Bild 6)

The discrepancy between the model prediction and measurements for the oldest part of the diffusion zone is attributed to the presence of porosity (100 h) which provides a means for local stress relaxation. Nevertheless, the trend that decarburization leads to a local tensile stresses is predicted qualitatively to be correct. Deviations between model and measurement within the first 30 µm are associated with the compound layer, which is not taken into account in the present model.

The importance of taking the transformation of carbides into account is shown in the following example. Assuming that no carbides are transformed into nitrides, the volume change accompanying the precipitation of MN is shown in Figure 10. Maximum volume changes of 3.80 % and 4.39 % are obtained (Figure 10), as compared to 1.32 % and 0.86 %, respectively (see Figure 8b). Consequently, a maximum calculated compressive residual stress of nearly – 350 MPa would result, which represents a clear overestimation of the experimental residual stresses (Figure 9). This example illustrates that the assumption of the transformation of carbides into nitrides and cementite as well as the growth of carbides ahead of the nitriding front are essential considerations in the development of residual stress in the nitride case.

The excellent correspondence between model and experiment as illustrated by Figure 9 strongly suggests that the generation and relaxation of stress in the present model alloy find their origins in the composition-induced evolution of the microstructure and associated transformations. The lower maximum compressive stress in a deep nitrided case (100 h) as compared to the higher maximum compressive stress in a shallow nitrided case (10 h) is a consequence of the growth of carbides ahead of the nitriding front, which removes Cr atoms from solid solution in ferrite. As a result fewer Cr atoms are available for direct nitride formation, and associated smaller compressive stress, and more carbon is released for grain boundary ferrite development, giving more stress relaxation. The deeper the nitrided case, the more pronounced this effect becomes, because the longer time is available for growth of the carbides ahead of the nitriding front as compared to growth of the diffusion zone.

The present work indicates that, provided that an accurate model is developed to predict the evolution of carbon and nitrogen concentration-depth profiles during nitriding, a fairly accurate prediction of the residual stress distribution can be obtained.

5 Conclusions

The microstructural evolution in the nitrided case of a model alloy Fe-3wt.%Cr-0.35wt.%C was characterized. Observations show that the transformation of initial carbides involves the precipitation of cementite and dissolution into ferrite. It results in a non-negligible decrease (relaxation) of the volume change accompanying the precipitation of nitrides from alloying elements in solid solution. The depletion of carbon from the diffusion zone close to the surface involves first a volumetric unloading due to the decrease of precipitate volume and the development of porosity along ferrite grain boundaries; these porous grain boundaries are (partly) in direct contact with the nitriding atmosphere and can locally lead to the development of γ'-Fe_4N along grain boundaries in the diffusion zone. An accumulation of carbon atoms ahead of the nitriding front is associated with growth of initially present (alloying element containing) carbides. Consequently, rather than the development of nitrides from alloying elements in solid solution in the diffusion zone as occurring in an early stage of nitriding, at larger depth the transformation of carbides into nitrides becomes dominant. Accordingly, the maximum compressive stress that is obtained in a deep diffusion zone is lower than the maximum compressive stress obtained in a shallow diffusion zone.

A model involving the assumption of local equilibrium for the actual composition at a certain depth and a self-consistent mechanical model, allows an accurate prediction of the residual stress depth profile.

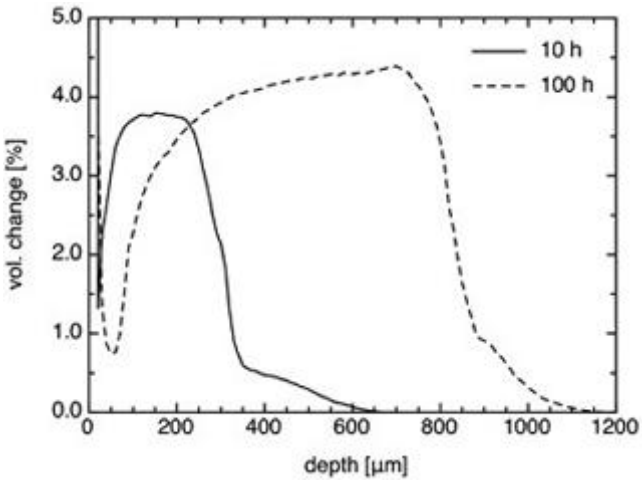

Fig. 10. Calculated volume changes accompanying the precipitation of nitrides during nitriding of Fe-3wt.%Cr-0.35wt.%C at 550 °C for 10 h and 100 h. No carbide transformation was taken into account

Bild 10. Volumenvariationen der Nitride während des Nitrierens einer Fe-3wt.%Cr-0,35wt.%C-Legierung bei 550 °C nach 10 h und 100 h; die Karbidumwandlung wurde nicht berücksichtigt

The authors acknowledge Aubert & Duval (Eramet Group) and the Safran Group for their support, as well as CP2M laboratory (Paul Cézanne University, Marseille, France) for TEM investigations and the Pprime Institute (University of Poitiers, France) for GDOES analysis.

References

1. *Kolozsvary, Z.:* Residual Stresses in Nitriding. In: Handbook of residual stress and deformation of steel, *Totten, G.; Howes, M.; Inoue, T.* (eds.); ASM Int., Materials Park/Ohio, 2002, pp. 209-219
2. *Mittemeijer, E. J.:* The relation between residual macro- and microstresses and mechanical properties of case-hardened steels. In: Case-hardened Steels: microstructural and residual stress effects. Proc. Symp. of the 112th AIME annual meeting, 03.09.1983, Atlanta/USA. D. E. Diesburg (Ed.), the Metallurgical Society of AIME, Warrendale/USA, 1984, pp. 161-187
3. *Barrallier, L.; Barralis, J.:* On origin of residual stresses generated by nitriding treatment on alloy steels. Proc. 4th Int. Conf. on Residual Stresses, ICRS4, June 8-10, 1994, Baltimore/USA. Soc. for Experimental Mechanics, Inc., Bethel, Conn./USA, 1994, pp. 498-505
4. *Girodin, D.; Moraux, J. Y.:* L'acier 32CrMoV13 nitruré profond pour applications aéronautiques. Proc. french-german Conf. on 'Nitrieren/Nitruration', 10-12.04.02 in Aachen. ATTT/AWT/SVW/VWT, 2002, pp. 295-306
5. *Barralis, J.; Castex, J.; Chaize, J. C.:* Influence des conditions de traitement sur la distribution des phases et des contraintes résiduelles dans les couches nitrurées. Mémoires et Etudes Scientifiques – Revue de Métallurgie *83* (1986) 12, pp. 629-642
6. *Vives Diaz, N. E.; Schacherl, R. E.; Zagonel, L. F.; Mittemeijer, E. J.:* Influence of the microstructure on the residual stresses of nitrided iron-chromium alloys. Acta Mater. *56* (2008) 6, pp. 1196-1208

7. *Buchhagen, P.; Bell, T.:* Simulation of the residual stress development in the diffusion layer of low alloy plasma nitrided steels. Comput. Mater. Sci. *7* (1996) 1-2, pp. 228-234
8. *Van Wiggen, P. C.; Rozendaal, H. C. F.; Mittemeijer, E. J.:* The nitriding behaviour of iron-chromium-carbon alloys. J. Mater. Sci. *20* (1985), pp. 4561-4582
9. Locquet, J. N.; Barrallier, L.; Soto, R.; Charai, A.: Complete TEM investigation of nitrided layer for a Cr alloy steel. Microscopy Microanalysis Microstructures *18* (1997) 12, pp. 335-352
10. *Oettel, H.; Schreiber, G.:* Eigenspannungsbildung in der Diffusionszone. Proc. AWT Conf. on ‚Nitrieren und Nitrocarburieren', 10-12.04.91, Darmstadt, 1991, pp. 139-151
11. Hirsch, T. K.; da Silva Rocha, A.; Ramos, F. D.; Strohaecker, T. R.: Residual stress-affected diffusion during plasma nitriding of tool steels. Metall. Mater. Trans. A *35* (2004), pp. 3523-3530
12. *Leroy, C.; Michel, H.; Gantois, M.:* Transformation of (Cr,M)7C3-type carbides during nitriding of chromium alloyed steels. J. Mater. Sci. *21* (1986), pp. 3467-3474
13. Jegou, S.; Barrallier, L.; Kubler, R.: Phase transformation and induced volume changes in a nitrided ternary Fe-3%Cr-0.345%C alloy. Acta Mater. *58* (2010), pp. 2666-2676
14. *Jegou, S.; Kubler, R.; Barrallier, L.:* On residual stresses development during nitriding of steel. Adv. Mater. Research *89-91* (2010), pp. 256-261
15. *Jegou, S.; Barrallier, L.; Kubler, R.:* Carbon diffusion induced stress relaxation during gas nitriding of a ternary Fe-3%Cr-0.345%C alloy. Under preparation, 2011
16. *Castex, L.; Lebrun, J. L.; Maeder, G.; Sprauel, J. M.:* Détermination des contraintes résiduelles par diffraction des rayons X. Ecole Nationale superieure d'Arts et Métiers, series: Publications Scientifiques et Techniques 22, 1981
17. *Somers, M. A. J.:* Modelling nitriding of iron: from thermodynamics to residual stress. J. Phys. IV *104* (2004) 104, pp. 21-33
18. *Rougier, Y.; Stolz, C.; Zaoui, A.:* Self-consistent modelling of elastic-viscoplastic polycrystals. Mechanics of Solids *318* (1994), pp. 145-151
19. JCPDS-International Center for Diffraction Data PDF-2, 2002